REPORT DOCUMENTATION PAGE

Form Approved
OMB No. 0704-0188

1. REPORT DATE *(DD-MM-YYYY)*	**2. REPORT TYPE**	**3. DATES COVERED** *(From - To)*
10/19/2012	Final Report	08/15/2009 to 08/4/2012

4. TITLE AND SUBTITLE
Novel Flexible Plastic-Based Solar Cells

5a. CONTRACT NUMBER
FA95500910361

5b. GRANT NUMBER

5c. PROGRAM ELEMENT NUMBER

6. AUTHOR(S)
Paras N. Prasad

5d. PROJECT NUMBER

5e. TASK NUMBER

5f. WORK UNIT NUMBER

7. PERFORMING ORGANIZATION NAME(S) AND ADDRESS(ES)

SUNY at Buffalo
ILPB
427 NSC Building
Buffalo NY 14260

8. PERFORMING ORGANIZATION REPORT NUMBER

9. SPONSORING / MONITORING AGENCY NAME(S) AND ADDRESS(ES)
USAF, AFRL
AF Office of Scientific Research
875 N. Randolph St RM 3112
Arlington VA 22203

10. SPONSOR/MONITOR'S ACRONYM(S)

11. SPONSOR/MONITOR'S REPORT NUMBER(S)
AFRL-OSR-VA-TR-2012-1212

12. DISTRIBUTION / AVAILABILITY STATEMENT

DISTRIBUTION A: APPROVED FOR PUBLIC RELEASE

13. SUPPLEMENTARY NOTES

14. ABSTRACT

Our scientific efforts in this project focused on the development of efficient solution-processing for solid state photovoltaic cells by spin-coating and spraying techniques, to produce broad-band light harvesting hybrid solar cells with bulk and layered heterojunction of inorganic semiconductor nanocrystals (NCs) and hole transporting polymers. Specifically, we achieved significant progress in fabrication and characterization of three different types of solar cells: 1) Synthesis of hole transporting low band gap polymers, development of ligand exchange in a nanocomposite, and fabrication of hybrid bulk heterojunction photovoltaic cell using a blend film of polymer-inorganic NCs, 2) Fabrication of newly designed hybrid solar cells that are composed of a electron transport layer (TiO_2), a light sensitizing layer (NCs), and a hole transport layer (polymer), 3) Development of thin film solar cells using low-cost spray technique and performance enhancement of its hybrid device. Photovoltaic characteristics were evaluated. The result showed the high performance of ~6% power conversion efficiency for solar cell type 2 above.

15. SUBJECT TERMS

16. SECURITY CLASSIFICATION OF:			**17. LIMITATION OF ABSTRACT**	**18. NUMBER OF PAGES**	**19a. NAME OF RESPONSIBLE PERSON**
a. REPORT	**b. ABSTRACT**	**c. THIS PAGE**			**19b. TELEPHONE NUMBER** *(include area code)*

Standard Form 298 (Rev. 8-98)
Prescribed by ANSI Std. Z39.18

TABLE OF CONTENTS

LIST OF FIGURES

GLOSSARY

P3HT	Poly(3-hexyl thiophene)
PCBM	[6,6]-Phenyl C-61-butyric acid methyl ester fullerene
NCs	Nanocrystals
TiO_2	Titanium dioxide
V_{OC}	Open-circuit voltage
PAG	Photoacid generator
t-Boc	*tert*-Butoxycarbonyl
J_{SC}	Short-circuit current density
ITO	Indium tin oxide
I-V	Current-voltage
Al	Aluminum
FF	Fill factor
PEDOT:PSS	Poly(3,4-ethylenedioxythiophene):Poly(styrenesulfonate)
QD	Quantum dot
PCE	Power conversion efficiency
OA	Oleic acid
TOPO	Trioctylphosphine oxide
FTO	Fluorine doped tin oxide

NOVEL FLEXIBLE PLASTIC-BASED SOLAR CELLS

1.0 INTRODUCTION

Polymer solar cells have attracted significant attention due to their advantages such as low cost, light weight, solution-processabillity, and facile fabrication to a large-area and flexible device. So far, the heterojuction of conjugated polymer (e.g. P3HT, poly(3-hexyl thiophene)) and soluble fullerene derivative (e.g. PCBM, [6,6]-phenyl C-61-butyric acid methyl ester fullerene) has produced power conversion efficiency up to 5~6%. To date, a variety of low band gap polymers have been investigated to exhibit PCE as high as 8~9% with a PCBM derivative (PC71BM). As a replacement of a typical organic electron acceptor (PCBM) in polymer solar cells, inorganic semiconducting nanocrystals have been investigated because of higher electron mobility, high electron affinity, and good chemical stability, which can be combined with the flexibility of a polymeric form. Furthermore, band gap tuning of nanocrystals by quantum confinement effects can compensate the limited light harvesting of polymer easily by blending two components to extend the absorption range, resulting in broad band harvesting of sun light.

During the period covered by this report, our scientific efforts have focused on the development of efficient solution-processing for solid state photovoltaic cells by spin-coating and spraying techniques, to produce broad-band light harvesting hybrid solar cell with bulk and layered heterojunction of inorganic semiconductor nanocrystals (NCs) and hole transporting polymers. Specifically, we have achieved significant progress in three different areas: 1) Synthesis of hole transporting low band gap polymers, development of ligand exchange in a nanocomposite, and fabrication of hybrid bulk heterojunction photovoltaic cell using a blend

film of polymer-inorganic NCs, 2) Fabrication of newly designed hybrid solar cells that are composed of a electron transport layer (TiO_2), a light sensitizing layer (NCs), and a hole transport layer (polymer), 3) Development of thin film solar cells using low-cost spray technique and performance enhancement of its hybrid device. Finally, we includ some results in polymer and small molecule solar cells with improved V_{OC}.

2.0 DISCUSSION OF RESULTS

2.1 Inorganic nanocrystal-polymer hybrid bulk heterojunction solar cells

2.1.1 Development of photopatterable NCs and their application in bulk heterojunction solar cells

We have developed various photopatterable NCs by functionalizing the surface of the NCs with optically and thermally cleavable ligand; *tert*-butyl *N*-(2-mercaptoethyl) carbamate. As given in Figure 1, micropatterned structures using newly developed NCs have been successfully demonstrated by means of *in-situ* photochemical reaction. In this scheme, the *t*-butoxycarbonyl (*t*-BOC) group of this carbamate ligand can be removed upon irradiation by UV light in the presence of a photoacid generator (PAG). This concept of chemical amplification leads to a drastic reduction of the dispersibility of the nanocrystals, enabling a solvent-selective development process after photopatterning.

Furthermore, our ligand deprotection strategy has been extended to polymer-inorganic nanocrystal (NC) hybrid solar cells consisting of a hole-conducting conjugated polymer and inorganic semiconducting quantum dots. Generally, it is necessary to perform ligand exchange

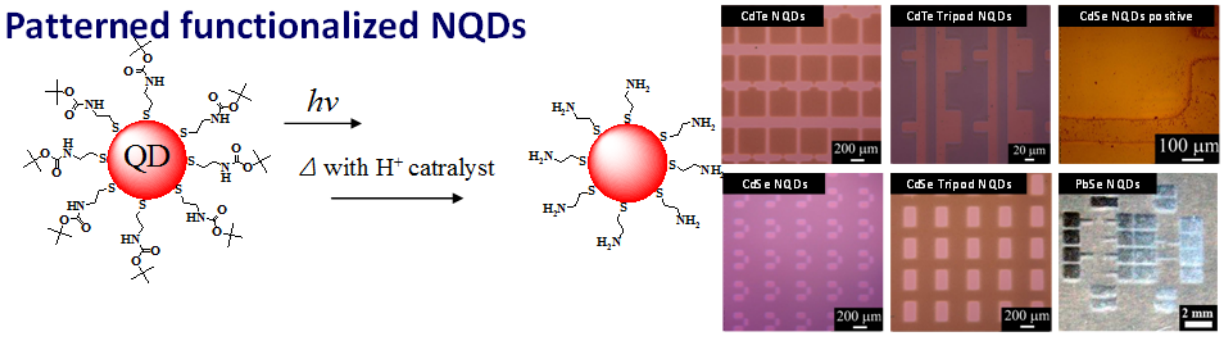

Figure 1: Schematic illustration of the photo-deprotection of *t*-Boc moiety in *tert*-butyl *N*-(2-mercaptoethyl)carbamate ligand linked to the surface of the nanocrystals, and its photopatterns.

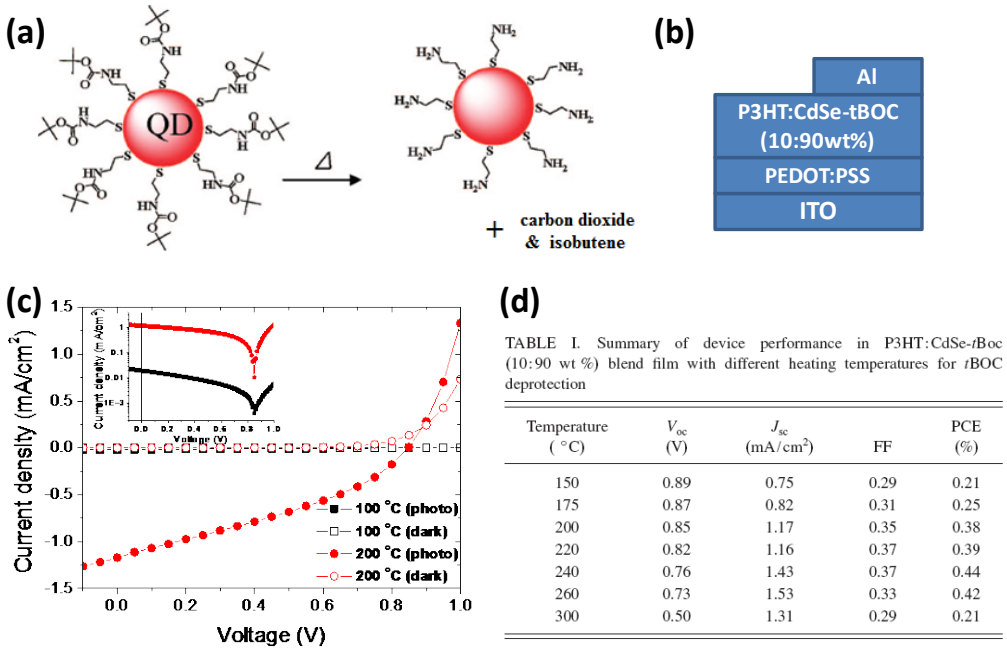

(d)

TABLE I. Summary of device performance in P3HT:CdSe-*t*Boc (10:90 wt %) blend film with different heating temperatures for *t*BOC deprotection

Temperature (°C)	V_{oc} (V)	J_{sc} (mA/cm^2)	FF	PCE (%)
150	0.89	0.75	0.29	0.21
175	0.87	0.82	0.31	0.25
200	0.85	1.17	0.35	0.38
220	0.82	1.16	0.37	0.39
240	0.76	1.43	0.37	0.44
260	0.73	1.53	0.33	0.42
300	0.50	1.31	0.29	0.21

Figure 2: (a) Schematic illustration of thermal deprotection of *t*-Boc moiety in *tert*-butyl *N*-(2-mercaptoethyl)carbamate ligand linked to the surface of the nanocrystals, (b) the device configuration, (c) Current density-voltage characteristics of the photovoltaic devices consisting of ITO/PEDOT:PSS/P3HT:CdSe-*t*BOC (10:90 wt %) /Al at heat treatment temperatures of 100 and 200 °C, and (d) the summary of photovoltaic performance at different heating temperature.

on the as-prepared NCs since they typically are shielded by long alkyl chain ligands, such as trioctylphosphine oxide (TOPO) and oleic acid (OA), which act as insulating layers. In this work, we demonstrated a significant improvement in the performance of a photovoltaic cell by *in-situ*

thermally shortening of ligand in a nanocomposite of poly (3-hexylthiophene) (P3HT) and carbamate ligands functionalized CdSe nanorods. Under controlled heat treatment conditions, the *t*-BOC group in this carbamate ligand releases isobutene and carbon dioxide. It has been demonstrated that the resulting shortened ligands on the SNCs lead to enhancement of charge generation and transport in thin film devices. As a result, the short circuit-current density (J_{SC}) was increased by 61 times and the power conversion efficiency (PCE) was enhanced by almost two orders of magnitude after heat treatment at 200 ^{o}C. (See Figure 2) The device performance was systematically investigated as a function of the heating temperature. Therefore, this thermal deprotection strategy for SNCs offers a simple and straightforward route to improve overall device performance which would be very applicable for polymer/NC hybrid photovoltaic devices.

2.1.2 Post chemical treatment for ligand modification in P3HT-PbS photovoltaics

It is well known that pre-ligand exchange for CdSe nanocrystals using pyridine is necessary for photovoltaic devices where a shortening of the ligands and the surrounding nanocrystals leads to better exciton dissociation between polymer and nanocrystal, as well as improved interparticle charge transport. In case of PbS, however, the pyridine exchange approach is inefficient due to lack of solubility, leading to precipitation of the PbS nanocrystals after pyridine treatment. In this work, we presented a methodology for a versatile and facile ligand exchange by post fabrication chemical treatment in PbS nanocrystal: poly(3-hexylthiophene) (P3HT) hybrid composite films. We reported considerable improvement of the photovoltaic performance after post chemical treatment using acetic acid to produce PbS nanocrystals surrounded by short-length ligands. (See Figure 3) This ligand exchange from oleic acid to acetic acid was monitored by FT-IR spectroscopy. A better excitonic interaction for charge generation at the improved interfacial

contact in blended film after treatment was also confirmed by transient decay of photoluminescence. Finally, annealing induced morphological and photovoltaic performance changes in the resulting composite films were investigated as a function of annealing time. However, this device efficiency would be relatively low, due to inefficient carrier generation by a poor type-II heterojunction. For example, there is a small energy difference between the valence band (5.0 ~5.2 eV) of PbS and the highest occupied molecular orbitals (HOMO) (5.1 eV) of P3HT. Thus it is necessary to develop an ideal π-conjugated polymer with well-matched energy levels for NCs to improve exciton dissociation.

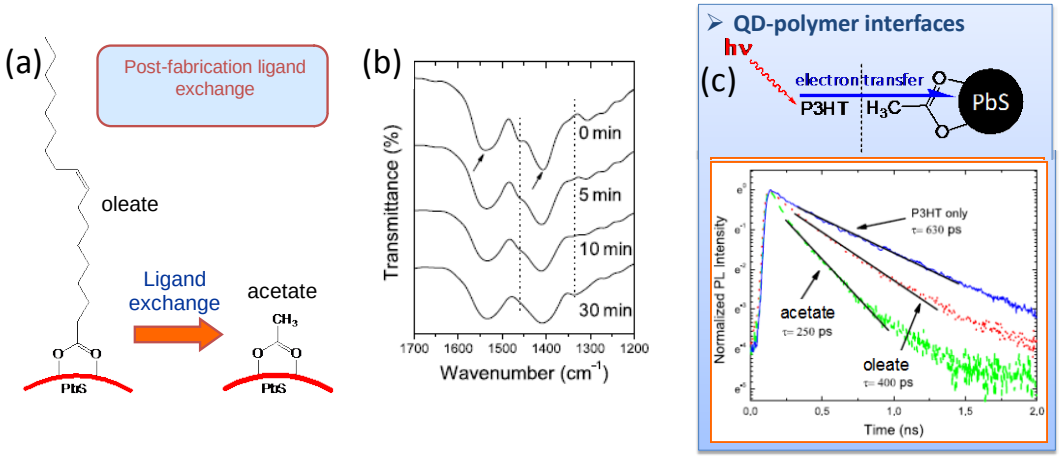

Figure 3: (a) Schematic illustration of post-ligand exchange using acetic acid, (b) FT-IR spectra of PbS nanocrystal as a function of the treatment time under acetic acid solution (0.01 M) in acetonitrile, and (c) Normalized time-resolved photoluminescence decay of P3HT only (blue), as well as the untreated (red) and the treated (green) P3HT:PbS film (50:50 wt%), respectively.

2.1.3Efficient heterojunction photovoltaic cell utilizing nanocomposites of lead sulfide nanocrystals and a low band gap polymer

Considering a need for improved exciton dissociation with PbS NCs, as discussed earlier, we designed and synthesized a low band gap polymer as shown in Figure 4. Using this polymer with absorption maximum of ca. 780 nm, we fabricated a simple and efficient hybrid solar cell

consisting of NIR-absorbing PbS NCs and a low band gap polymer, as shown in the schematic device configuration (Figure 5).

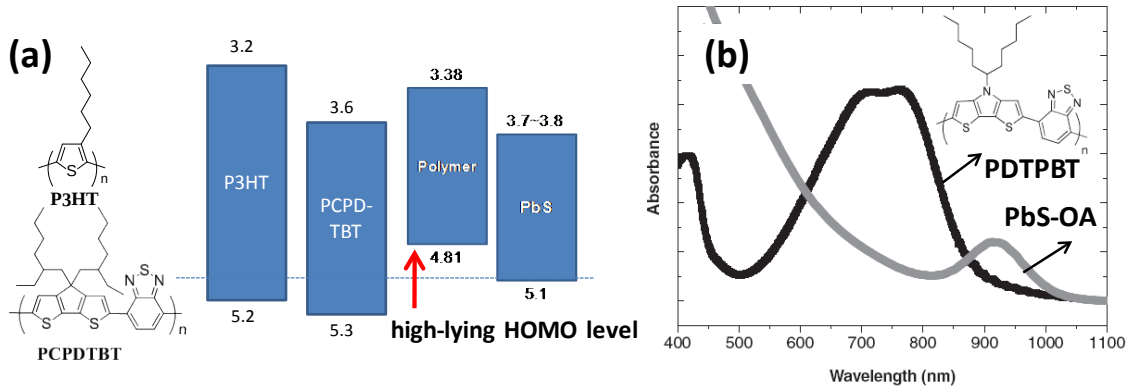

Figure 4: (a) Schematic illustration of band alignment for exciton dissociation between PbS NCs and polymers, and (b) Absorption spectra of PDTPBT film (black line), OA-capped PbS nanocrystals dispersed in *n* -hexane in a 1 cm cuvette (gray line). The inset shows the molecular structure of the PDTPBT polymer.

A 150 nm PDTPBT:PbS-OA (10:90 wt%) blend film was deposited on the top of the PEDOT:PSS layer (~40 nm) by spin-coating, followed by chemical treatment. Post ligand exchange was carried out by deposition of 1,2-ethanedithiol (EDT) solution in acetonitrile (AcCN) onto the PDTPBT:PbS-OA blend film and spin-coating to replace the oleic acid ligand with EDT. Subsequent washing was performed using pure AcCN and *n*-hexane to remove the exchanged oleic acid and any residual EDT. Next, the TiO_2 layer (~40 nm) was deposited onto the treated PDTPBT/PbS blend film by spincoating of TiO_2 NCs, which were prepared by a non-hydrolytic sol-gel method. Finally, the device fabrication was completed by thermal evaporation of LiF (~1nm) and Al (35nm), followed by evaporation of Ag (60nm).

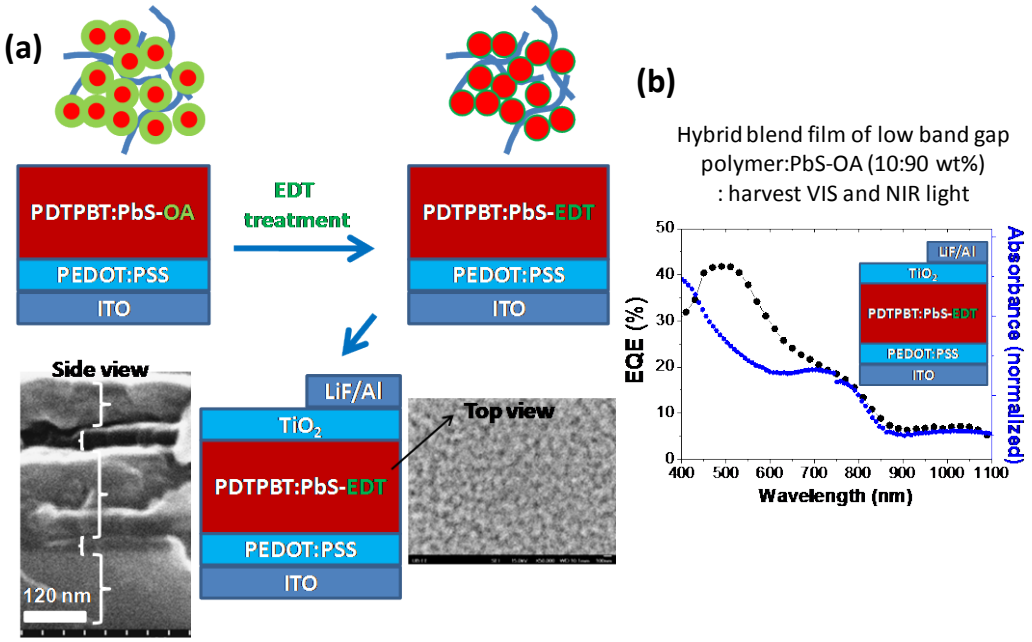

Figure 5: (a) Schematic diagram of the fabrication procedure and the device structure. The SEM image shows the side view of the device and the surface morphology of the EDT-treated blend film of PDTPBT/PbS (10/90wt%). (b) Plots of the absorption spectrum of the EDT-treated blend film of PDTPBT/PbS (10/90wt%) and the EQE spectrum of the blend device.

The resulting device exhibited a broad spectral response as given in the EQE spectrum in Figure 5. In the EQE spectrum, there is a significant contribution of the PDTPBT polymer in the range of 600~850 nm. Also, this EQE extends to 1100 nm, primarily due to the absorption of the PbS NCs. As a consequence, a combination of low band gap polymer and the NIR absorbing PbS NCs gives rise to a broad response covering from the UV to the NIR spectral range. Figure 6 shows the *I-V* characteristics of the PDTPBT/PbS blend devices after EDT treatment, measured under AM1.5G illumination at 100 mW/cm^2. The device without a TiO_2 layer exhibits a J_{sc} of 13.6 mA/cm^2, V_{oc} of 0.36 V, and a FF of 43 %, resulting in an overall PCE of 2.07 %. Moreover, the insertion of a TiO_2 layer between the blends and metal resulted in additional improvement in J_{sc} (increase of 9.2%) and FF (increase of 14.5%), yielding a PCE of 2.70 %. A thin TiO_2 interlayer acting as a hole blocking buffer layer could facilitate efficient electron transfer toward

the metal. In addition, the addition of the TiO_2 layer resulted in a decrease in series resistance (from 10.7 to 6.3 ohm cm^2), but with no large variation in shunt resistance, implying that the TiO_2 interlayer is capable of reducing the contact resistance in device.

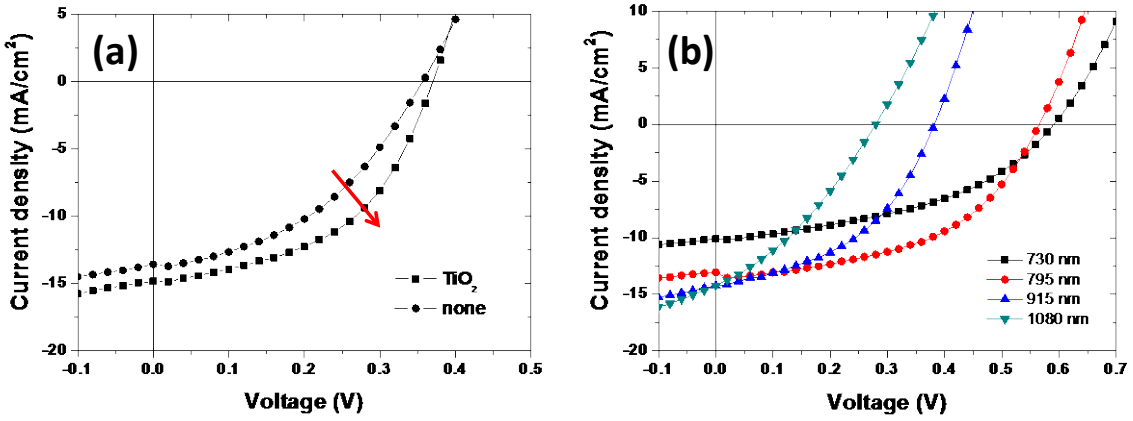

Figure 6: (a) *I–V* characteristic of the PDTPBT/PbS (10/90wt%) blend device in the presence (square) and the absence (circle) of the TiO 2 layer under AM1.5G (100 mW/cm^2) illumination. The PbS NCs with the first exciton absorption wavelength of 920 nm were used. (b) *I–V* characteristic of the device using PbS NCs with different first excitonic absorption peaks in the ITO/PEDOT:PSS/PDTPBT:PbS(10:90 wt%)/TiO_2 /LiF/Al device.

To gain more insight into the photovoltaic performance as a function of the optical band gap of the PbS NCs, we compared hybrid devices fabricated from the PbS NCs with first exciton wavelengths at 730, 795, 915, and 1080 nm, respectively, as shown in **Figure 6.** It is found that V_{oc} increases significantly whereas J_{sc} decreases, as the first exciton wavelength of PbS NCs decreases. The FF shows the highest value when the PbS NCs with the first exciton peak at 795 nm is used. The resultant photovoltaic behavior as a function of the band gap (E_g) of the PbS NCs exhibits a trade-off between V_{oc} and J_{sc}. As a result, the optimum condition for PCE was obtained with the hybrid blend device using the PbS NCs with a first excitonic peak at 795 nm. In particular, this photovoltaic performance can be primarily attributed to an increase in V_{oc}. Therefore, among the hybrid devices fabricated here, the best power conversion efficiency of

3.78 % was obtained with the polymer blend film having PbS NCs with the first excitonic peak at 795 nm. We believe that this efficiency is the highest among those hybrid bulk heterojunction cells based on polymer and PbS (or PbSe) NCs reported in the literature.

2.2Efficient PbS NCs- TiO_2 film heterojunction solar cell with a hole transporting polymer layer

To enable broadband absorption in the visible and near infrared (NIR) wavelengths, PbS and PbSe NCs have been widely investigated in a variety of device architectures, including NC-polymer hybrid solar cells, NC Schottky solar cells, and NC-sensitized solar cells. Recent photovoltaic devices utilizing heterojunctions between p-type PbS NC films and n-type metal oxides such as ZnO and TiO_2 have reached promising power conversion efficiencies of 3.0~6.0%. Very recently, there have been several demonstrated approaches for improving the efficiency by simply modifying the PbS NCs-Au metal interface through the insertion of a hole extraction

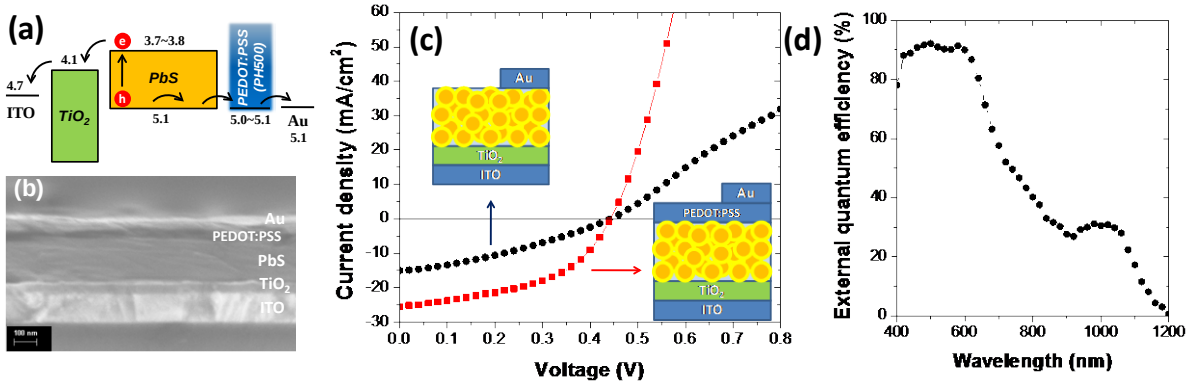

Figure 7: (a) Energy band diagram of the device structure, (b) The SEM image of the cross section of the devices, (c) I-V characteristics of the TiO2-PbS heterojunction device without (black) / with (red) a PEDOT:PSS layer under AM1.5G (100 mW/cm^2) illumination, and (d) EQE spectrum of the TiO2-PbS heterojunction device with a PEDOT:PSS layer.

layer like a transition metal oxide (MoO_x and V_2O_x). It was thus noted that a hole-injection barrier, resulting from the Schottky barrier at the PbS NC/metal interface, could impede hole-extraction toward the metal. In this respect, we reported a highly efficient hybrid nanostructured solar cell based on a TiO_2-PbS NC heterojunction with a hole transporting and an electron blocking polymer layer (See Figure 7). The incorporation of the PEDOT:PSS layer between the PbS NCs and the Au metal enhances the photocurrent significantly due to the elimination of the Schottky junction and resulting efficient hole extraction. In addition, we found that the deposition of PEDOT:PSS on the surface of the PbS NC film has the beneficial effect of reducing the concentration of surface defects ($PbSO_4$, a recombination center) present on the surface of PbS NC films and thus, improving the electrical contact. The device with the PEDOT:PSS layer also exhibited a relatively better air stability under solar illumination, as compared with the device without PEDOT:PSS. As a result, the best-performing device yielded a power conversion efficiency (PCE) of 5.4 % under AM1.5G (100 mW/cm^2) illumination. Therefore, a better understanding of the multiple effects produced by the PEDOT:PSS layer in our TiO_2-PbS NC heterojunction cell is critical to building new PbS-based solar cell devices with improved photovoltaic performance.

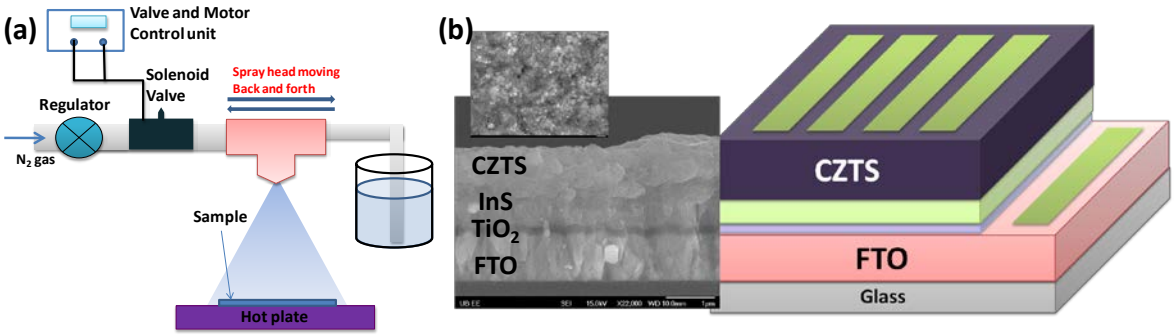

Figure 8: (a) Schematic illustration of spray pyrolysis technique for thin film solar cells, and (b) Cross-section SEM micrograph and device structure of FTO/TiO_2/In_2S_3/ C_2ZTS_4 solar cell; the inset shows the surface morphology of sprayed C_2ZTS_4 layer (scale bar : 1µm).

2.3Thin film (CZTS) solar cell with the spray pyrolysis technique

We investigated the Cu_2ZnSnS_4 (C_2ZTS_4) thin film solar cell with the spray pyrolysis technique under the inverse stacking structure of a conventional $CuInGaSe_2$ ($CIGS_2$) solar cell. All layers are sprayed on a fluorine doped tin oxide (FTO) substrate at different temperatures, as given in Figure 8. The power conversion efficiency (PCE) is 4.4% with 410mV of open circuit voltage (V_{OC}), 30.4mA/cm^2 of short circuit current density (J_{SC}) and 35.3% of fill factor (FF) under AM 1.5G illumination condition. We found that the crossover phenomenon in current-voltage (I-V) curve was affected by the spraying temperature of the In_2S_3 buffer layer. The optimum growth temperature for the best solar cell performance is 360 ˚C for both the In_2S_3 buffer and the C_2ZTS_4 absorber layers with a low crossover effect.

2.4 Polymer and small molecule solar cells for an improved V_{OC}

2.4.1 Enhanced performance of organic photovoltaic cells fabricated with a methyl thiophene-3-carboxylate-containing alternating conjugated copolymer

Increasing of power conversion efficiency in polymer bulk-heterojunction solar cell has been recently achieved by two approaches: 1) improving J_{SC} by more light-absorption of a low band gap polymer due to extended spectral response, and 2) improving V_{OC} by controlling a HOMO energy level of the polymer in a bulk-heterojunction with PCBM. In this respect, we also designed and synthesized for polymer solar cells (PSCs) using a new donor-acceptor copolymer, containing benzodithiophene (BDT) and methyl thiophene-3-carboxylate (3MT) units for improving V_{OC}. The 3MT unit was used as an electron acceptor unit in this copolymer to provide a lower highest occupied molecular orbital (HOMO) level for obtaining polymer solar cells with a higher open-circuit voltage (V_{OC}). The resulting bulk heterojunction PSC made of the copolymer and [6,6]-phenyl-C71-butyric acid methyl ester (PC71BM) exhibited a power conversion effi ciency (PCE) up to 4.52%, a short circuit current (J_{SC}) of 10.5 mA/cm^2, and a V_{OC} of 0.86 V. (See Figure 9)

2.4.2 Effect of alkyl side-chain in a methyl thiophene-3-carboxylate-containing alternating conjugated copolymer on the device performance

Four alkyl-substituted thiophene-3-carboxylate containing donor-acceptor (D-A) copolymers were designed, synthesized, and characterized. (See Figure 9) Thiophene-3-carboxylate was used as a weak electron acceptor unit in the copolymers to provide a deeper highest occupied molecular orbital (HOMO) level for obtaining a higher open-circuit voltage in polymer solar cells (PSCs). The resulting bulk heterojunction PSCs, made of the copolymers and [6,6]-phenyl-C71-butyric acid methyl ester (PC71BM), exhibited different short circuit currents (J_{SC}s) and

open-circuit voltages (V_{OC}s), depending on the length of the alkyl side-chain in the thiophene-3-carboxylate unit. Among all fabricated photovoltaic (PV) devices, PC2:PC71BM (1:1 wt. ratio) showed the highest efficiency with the highest J_{SC} of 10.5 mA/cm^2. Although PC5:PC71BM (1:1) displayed the highest V_{OC} of 0.93 V, the device efficiency was observed to be poor, which is due to poor nanophase segregation. This comparison shows that the side-chain of thiophene carboxylate in these copolymers plays a very important role in the device efficiency.

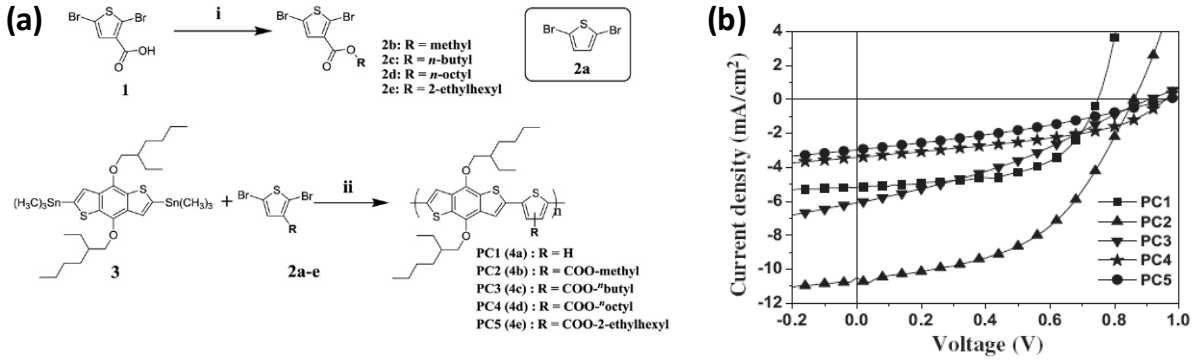

Figure 9: (a) Synthetic procedure and molecular structures of alkyl-substituted thiophene 3-carboxylate containing donor-acceptor (D-A) copolymers, and (b) Current density-voltage characteristics of PV devices based on copolymer:PC71BM (1:1 wt %) blends.

2.4.3Tricyanofuran-based donor–acceptor type chromophores for bulk heterojunction organic solar cells

Recently, solution-processed small molecular solar cells have been intensively studied due to several advantages like better reproducibility of synthesis and higher purity, as compared to polymer solar cells. In this work, we tried to apply a simple D-A dye of photorefractive chromophore into photovoltaic device with PCBM. Tricyanofuran-based small molecules were synthesized through Knoevenagel reaction with formyl heteroaromatic donating moieties and 2-cyanomethylene-3-cyano-4,5,5-trimethyl-2,5-dihydrofuran (TCF) as a strong acceptor. UV–vis

absorption demonstrated that the combination of TCF with donating units resulted in an enhanced intra-molecular charge transfer (ICT) transition, which led to long wavelength absorption in the chromophores. The absorption coefficients and the molecular energy levels of the chromophores could be tuned effectively by employing different donating groups. The chromophores were used in conjunction with [6,6]-phenyl-C61-butyric acid methylester (PC61BM) or [6,6]-phenyl-C71-butyric acid methylester (PC71BM) to fabricate organic heterojunction photovoltaic cells. This solution-processed bulk heterojunction (BHJ) solar cells exhibited a power conversion efficiency (PCE) of 2.44%, a short-circuit current density (J_{SC}) of 8.74 mA/cm^2, and an open-circuit voltage (V_{OC}) of 0.93V under simulated air mass 1.5 global irradiation (100mW/cm^2).

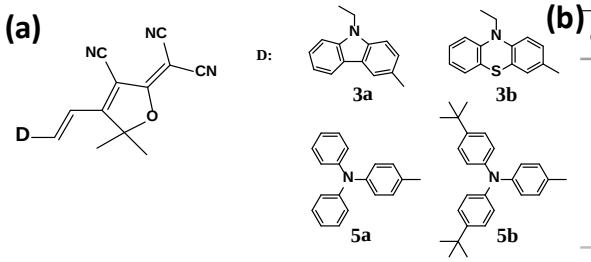

(b)

chromophores	Chromophore : PCBM [wt %]	J_{SC} [mA /cm^2]	V_{OC} [V]	*FF*	*PCE* [%]
3a	3a:$PC_{61}BM$ (1:3)	0.26	0.82	0.30	0.064
3b	3b:$PC_{71}BM$ (1:2)	6.01	0.85	0.29	1.47
5a	5a:$PC_{61}BM$ (1:1)	5.60	0.87	0.28	1.35
	5a:$PC_{71}BM$ (1:1)	7.42	0.85	0.28	1.77
	5a:$PC_{71}BM$ (1:2)	8.74	0.93	0.30	2.44
5b	5b:$PC_{71}BM$ (1:1)	1.11	0.87	0.28	0.27

Figure 10: (a) Molecular structures of tricyanofuran-based donor–acceptor type chromophores, and (b) Comparison of device characteristics of different chromophore:PCBM blend ratios.

3.0 CONCLUSIONS

During the period covered by this report, we developed efficient nanostructured solar cells based on a bulk and layered heterojunction of organic-inorganic hybrid materials. The device structure was fabricated by solution-processing using spin-coating and spraying techniques. Our scientific research efforts focused on the development of an efficient solid state photovoltaic cell utilizing

a broad light harvesting containing visible and NIR wavelength. Specifically, we have performed the fundamental studies on the following: i) preparation of nanocrystals acting as the infrared (IR)-absorbing photosensitizer to extend the spectral response, ii) synthesis of low band gap polymers and their band gap tuning, iii) development of the functional ligands and optimization of ligand exchange method for an improvement in the efficiency of charge generation in a hybrid nanocomposite (due to a better interfactial interaction between nanocrystals and polymer), and iv) development of spray pyrolysis technique for fabrication of nanocrystal-thin film. Considering all the parameters above, we fabricated nanostructured photovoltaic device and made significant progresses in three different device architectures as summarized in Figure 11.

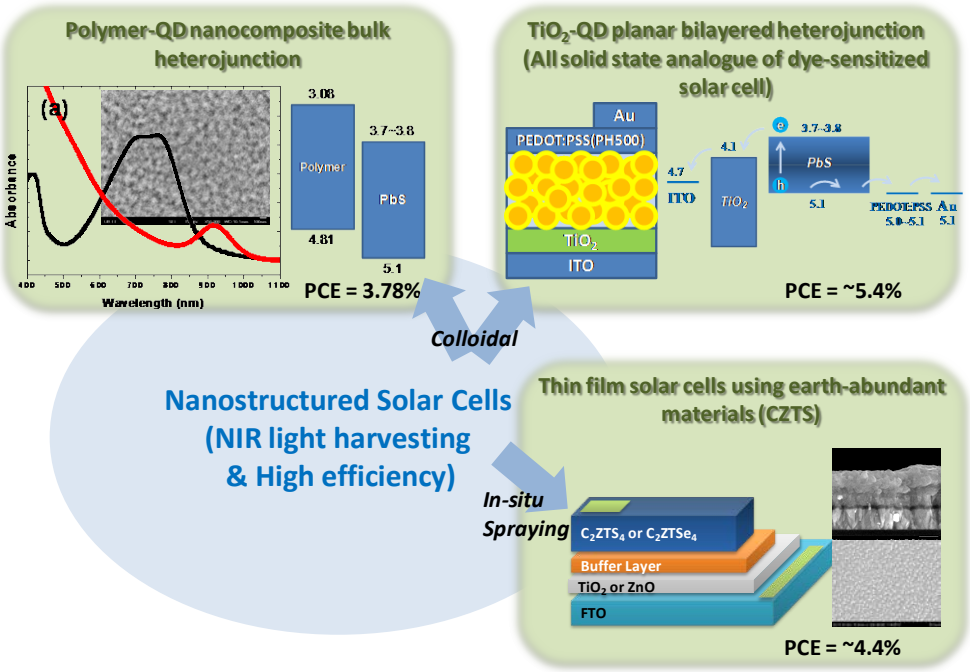

Figure 11: Summary of our research progress in efficient hybrid nanostructured solar cells utilizing NIR light harvesting

LIST OF PUBLICATIONS

1) Seo, J.; Kim, W. J.; Kim, S. J.; Lee, K.-S.; Cartwright, A. N.; Prasad, P. N. "Polymer Nanocomposite Photovoltaics Utilizing CdSe Nanocrystals Capped with a Thermally Cleavable Solubilizing Ligand", *Appl. Phys. Lett.*, **2009**, *94*, 133302.

2) Seo, J.; Kim, S. J.; Kim, W. J.; Singh R.; Samoc, M.; Cartwright, A. N.; Prasad, P. N. "Enhancement of Photovoltaic Performance In PbS Nanocrystal:P3HT Hybrid Composite Devices By Post Treatment-Driven Ligand Exchange", *Nanotechnology*, **2009**, *20*, 095202.

3) Kim, W. J.; Nyk, M.; Prasad, P. N. "Color-coded multilayer photopatterned microstructures using lanthanide (III) ions co-doped NaYF4 nanoparticles with upconversion luminescence for possible applications in security", *Nanotechnology*, **2009**, *20*, 185301.

4) Zhu, J.; Kim, W. J.; He, G. S.; Seo, J.; Yong, K.-T.; Lee, D.; Cartwright, A. N.; Cui, Y.; Prasad, P. N. "Enhanced Photorefractivity in a Polymer/Nanocrystal Composite Photorefractive Device at Telecommunication Wavelength", *Appl. Phys. Lett.*, **2010**, *97*, 963108.

5) Seo, J.; Cho, M. J.; Lee, D. H.; Cartwright, A. N.; Prasad, P. N. "Efficient hybrid photovoltaic cell utilizing nanocomposites of lead sulfide nanocrystals and a low-band gap polymer", *Adv. Mater*. **2011**, *23*, 3984.

6) Cho, M. J.; Seo, J.; Oh, H.; Jee, H.; Kim, W. J.; Hoang, M. H.; Choi, D. H.; Prasad, P. N. "Tricyanofuran-based donor-acceptor type chromophores for bulk heterojunction organic solar cells", *Sol. Energy Mater. Sol. cells*, **2012**, *98*, 71.

7) Cho, M. J.; Seo, J.; Kim, K. H.; Choi, D. H.; Prasad, P. N. “Enhanced performance of organic photovoltaic cells fabricated with a methyl thiophene-3-carboxylate-containing alternating conjugated copolymer”, *Macromole. rapid commun.* **2012**, *33*, 146.

8) Cho, M. J.; Seo, J.; Luo, K.; Kim, K. H.; Choi, D. H.; Prasad, P. N. “Polymer solar cells fabricated with 4,8-bis(2-ethylhexyloxy)benzo[1,2-*b*:4,5-*b′*]dithiophene and alkyl-substituted thiophene-3-carboxylate-containing conjugated polymers: Effect of alkyl side-chain in thiophene-3-carboxylate monomer on the device performance”, *Polymer* **2012,** *53*, 3835.

9) Seo, J.; Lee, D. H.; Cartwright, A. N.; Prasad, P. N. “Efficient PbS nanocrystal heterojunction solar cell employing thin TiO_2 films and a hole transporting polymer layer”, *submitted to Adv. Func. Mater.* (**2012**).

LIST OF PRESENTATIONS

1) Kim, W. J.; Kim, S. J.; Seo, J.; Sahoo, Y.; Cartwright, A. N.; Lee, K.-S.; Prasad, P. N. “Binding Characteristics of Surface Ligands on PbSe QDs and Impact on Electrical conductivity”, *Mater. Res. Soc. Symp. Proc.* **2009**, *1113*, F03/01-06.

2) Kim, S. J.; Kim, W. J.; Seo, J.; Cartwright, A. N.; Prasad, P. N. “Functionalized semiconductor nanocrystal quantum dots for patterned, multilayered photovoltaic devices”, *Mater. Res. Soc. Symp. Proc.* **2009**, *1121*, 66.

3) Lee, D.; Seo, J.; Kim, S. J.; Cartwright, A. N.; Prasad, P. N. "Trap Induced Limits of PCE in SILAR-based Solar Cell", *MRS* **2010**, Boston, MA.

4) Lee, D.; Seo, J.; Cartwright, A. N.; Prasad, P. N. “Fabrication of copper zinc tin sulfide (C_2ZTS_4) solar cells using spray chemical vapor deposition”, *SPIE Optics+Photonics* **2011**, San diego, CA.

5) Seo, J.; Cho, M. J.; Lee, D.; Cartwright, A. N.; Prasad, P. N., “Efficient heterojunction photovoltaic cell utilizing nanocomposites of lead sulfide nanocrystals and a low band gap polymer”, *SPIE Optics+Photonics* **2011**, San diego, CA.

6) Seo, J.; Lee, D.; Cartwright, A. N.; Prasad, P. N., “Improved Efficiency in a PbS nanocrystal heterojunction solar cell by employing a thin TiO_2 film and a hole transporting polymer layer”, *MRS* 2011, Boston, MA.